Hindawi
Shock and Vibration
Volume 2022, Article ID 5237381, 7 pages
https://doi.org/10.1155/2022/5237381

Research Article

Study on Dynamic Performance of Standard Sand Based on KTL Dynamic Triaxial Apparatus

Bo Li, Xiaofei Li, and Xueyang Xing

School of Architecture Engineering, Binzhou University, Binzhou 256600, China

Correspondence should be addressed to Xiaofei Li; lxf2011iem@126.com

Received 28 April 2022; Revised 13 May 2022; Accepted 17 May 2022; Published 28 May 2022

Academic Editor: Pengfei Wang

The determination of dynamic properties is of great scientific significance to the constitutive modeling and parameter determination of large deformation for sand liquefaction. For Fujian standard sand, a new high-precision KTL bidirectional dynamic triaxial test system was used to carry out liquefaction tests under equal consolidation and different equal amplitude cyclic stresses. The dynamic characteristics of Fujian standard sand, such as dynamic stress and dynamic strain test results, pore water pressure model, effective stress path, and stress-strain relationship curve, were studied. The main results are as follows: the whole vibration process of the sample could be basically divided into four stages: the greater the dynamic stress is, the easier the sample is to liquefy. With the increasing vibration times, the samples under different dynamic stress amplitudes meet the qualitative analysis of the first three stages of liquefaction; that is, the pore water pressure increases rapidly at the beginning of vibration, and the growth is stable in the middle stage. When the effective pore water pressure increases to 60 kPa, it begins to increase sharply and finally reaches the effective confining pressure, and then, the soil sample liquefies. The axial strain begins to accumulate in the compression direction and gradually increases. After liquefaction, the strain accumulates in the tensile direction in equal amplitude. During the whole vibration process, the axial strain of the sample can develop greatly in the tensile and compressive direction. Under the action of different cyclic stresses, the stress path of the soil sample tends to zero, and the rate of effective stress state varies greatly, indicating that the dynamic stress has a great influence on the dynamic liquefaction process of Fujian standard sand. In the dynamic triaxial test of standard sand, the difference in dynamic stress amplitude will lead to great changes in the stress-strain relationship curve. But it has little effect on the analysis of liquefaction dynamic characteristics of sand.

1. Introduction

Since the 1964 Niigata earthquake in Japan and the Alaska earthquake in the United States [1], the damage and impact of liquefaction on engineering structures and infrastructure have attracted extensive attention [2, 3]. In the Tangshan and Haicheng earthquakes in China, significant liquefaction occurred, causing great disasters. In recent years, with the development of soil dynamics theory and test technology, people have done a lot of research on liquefaction discrimination method [4], liquefaction theoretical analysis [5], influencing factors of liquefaction [6], and liquefaction prevention measures [7], but there are still some important problems that need to be explored.

The research on the constitutive characterization of soil mechanical properties during liquefaction is the core of sand liquefaction research [8]. Because of its strict theory and wide application, the elastic-plastic model has great potential for describing the failure mechanism of saturated sand under complex load [9]. There are many studies on the constitutive model of soil mechanical properties during liquefaction [10]. The Cambridge model proposed by Bigoni and Piccolroaz [11, 12] described the basic mechanical properties of saturated remolded soil. Li et al. [13] introduced the concept of initial anisotropy into the model for the first time to describe the anisotropy of soil. Zhang et al. [14, 15] established a cyclic fluidity model based on the modified Cambridge model, which well explained the

physical significance of different mechanical properties of different soil types. Ye et al. [16] presented the ts-cm model based on the transformed stress method, which considered the influence of intermediate principal stress and clarified the different mechanical properties of soil during compression and tension in the dynamic triaxial test. The above work excellently established the elastic-plastic constitutive model framework of large deformation of liquefied sand.

Performance design has become the development direction of engineering seismic design, which puts forward higher requirements for the simulation of seismic damage of liquefaction site. It is necessary to control the development and change of soil dynamic behavior in the process of liquefaction, and the stress-strain relationship of sand and the change law of pore water pressure are some of the key problems. Fu et al. [17] and Feng Dong et al. [18] proposed the incremental model of pore water pressure to calculate the pore water pressure under irregular load, but their models were derived from the theoretical formula. Sun and Yuan [19] proposed the pore water pressure increment model of Harbin sand under unequal consolidation by using the triaxial test, which was greatly limited in application.

In order to meet the requirements of performance design, the change process of soil shear strength under the increase of pore pressure is more and more needed for the problem of soil liquefaction, whether in the analysis of foundation strength and deformation or the calculation of soil ground motion. Based on the current knowledge [20], it can be seen qualitatively that the shear strength of Fujian standard sand would decrease with the increase of pore pressure, but the quantitative results are still few, which could not meet the above requirements. This is mainly due to the limitation of the function and accuracy of instruments and equipment in the previous experimental research, which is difficult to well describe the stress-strain hysteretic curve of soil in the process of liquefaction. The dynamic stress, dynamic strain, and effective stress path of the above soil are equivalent to the dynamic characteristic parameters of the soil. They are the key to control the dynamic behavior of the soil, which has important engineering significance for seismic design.

In this paper, a new high-precision two-way dynamic triaxial test system was used to carry out liquefaction tests under equal consolidation and different equal amplitude cyclic stresses. The dynamic characteristics of Fujian standard sand, such as dynamic stress and dynamic strain test results, pore water pressure model, effective stress path, and stress-strain relationship curve, were studied, which provides a basis for large deformation constitutive modeling of standard sand liquefaction and site dynamic response analysis under liquefaction.

2. Main Technical Indicators of KTL

The KTL bidirectional dynamic triaxial system of Binzhou University mainly consists of a dynamic triaxial host, triaxial pressure chamber, back pressure-volume pressure controller, dynamic confining pressure-volume pressure controller, dynamic control, and data acquisition system. Figure 1 shows its detailed composition. The technical indexes of the dynamic three-axis system are shown in Table 1.

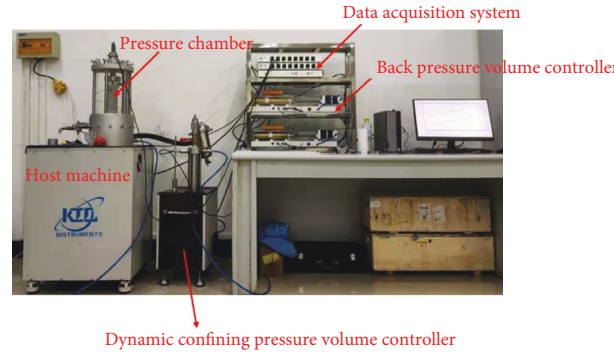

Figure 1: Composition of KTL dynamic triaxial system.

The KTL dynamic triaxial apparatus applies axial pressure by using the downloading type, integrates the triaxial pressure chamber with the axial dynamic actuator, and can apply the maximum dynamic load, deformation, and stress of 5 Hz. All equipment modules included in KTL dynamic triaxial system can be connected to the computer through USB. Various conventional geotechnical experiments can be completed by using KTL GeoSmartLab geotechnical comprehensive test software [21].

3. Test Scheme

The dimensions of soil samples in this test are Φ 50 mm × 100 mm. The soil sample used in the test is Fujian standard sand. The basic physical parameters of standard sand are shown in Table 2. The liquefaction probability of medium dense sand was high, so the soil sample with a relative density of 55% was used at room temperature. Three dynamic stress amplitudes (26 kpa, 33 kpa, and 41 kpa) were taken for the liquefaction test to study the variation law of liquefaction dynamic characteristics of standard sand.

The effective consolidation confining pressure of the test was 100 kPa, and the consolidation ratio was 1.0. The stress control mode was used for equal amplitude sine wave loading, and the loading frequency was 1 Hz. The test scheme is shown in Table 3.

4. Test Method

The test adopted the preparation method on the instrument. The soil sample preparation was carried out in strict accordance with the geotechnical test specification. The test process was divided into four parts: sample loading, saturation, consolidation, and vibration liquefaction test, just as follows.

(1) According to the relative density, the dry density of the sample was calculated to be 1.577 g/cm^3, and the quality of sand required for each sample was obtained. The sample was prepared by dry method and compacted in five layers with 20 mm for each layer, so as to ensure that the compaction number of each layer was basically the same.

Table 1: Technical index of the dynamic triaxial instrument.

Technical index	Index range and accuracy
Axial force	60 kN, ≤0.01%
Axial displacement	100 mm, ≤0.07%
Volume pressure controller	2 MPa, ≤0.15%
Pore pressure sensor	2 MPa, ≤1.5%
Chamber pressure	2 MPa, ≤0.1%
Working frequency	1–5 Hz

(2) After loading, the sample is saturated. Saturation is proposed to be divided into three saturation processes. The sequence was to pass CO_2 gas for 2 hours, then distilled water for 3 hours, and finally saturate through back pressure (the pressure difference of each stage was 30 kPa). When the measured pore water pressure coefficient $b \geq 0.98$, it is considered that the soil sample meets the saturation requirements.

(3) An effective consolidation confining pressure of 100 kPa is applied to the soil sample. After the consolidation is stable, the saturated sample is loaded through the dynamic test module. The change of pore pressure is monitored in real time during the loading process. When the pore water pressure reaches the effective confining pressure, it is considered that the sand is liquefied and the test is stopped. If the pore pressure does not reach the effective confining pressure, the dynamic stress stops after 1000 times of application.

5. Test Results

5.1. Typical Test Results and Dynamic Strength Test Results. Figure 2 shows the time history curves of stress, strain, and pore pressure U of Fujian standard sand under cyclic load with a dynamic stress amplitude of 33 kPa. It can be seen from Figure 3 that with the increased vibration times, the pore water pressure gradually increased and then stopped rising when reaching the confining pressure, and the strain gradually increased. The whole vibration process could be basically divided into four stages.

The first stage was the initial several cycles. In this stage, the amplitude of dynamic stress was stable, and the dynamic strain was from scratch. Some unstable particles moved to a relatively stable position, and the position adjustment occurs. Therefore, the growth rate of pore water pressure was fast. At the end of this stage, the effective pore water pressure was about 15 kPa. This stage was called the particle adjustment stage.

The second stage was the most important stage of the experiment. In this stage, the dynamic stress amplitude remained stable, the axial strain began to accumulate in the compression direction, and the growth rate of pore water pressure was stable. At the end of this stage, the effective pore water pressure was about 60 kPa. The stable accumulation of axial strain in this stage leads to the stable growth of pore water pressure, which was called the strain accumulation stage.

The third stage occurs in the later stage of the vibration process. In this stage, the number of cycles was small, the strain amplitude suddenly increased, and the axial strain also increased rapidly. At this time, the pore pressure also increased rapidly to equal the confining pressure, reaching liquefaction, and the soil basically lost its shear capacity. This stage was called the liquefaction stage. It should be noted that if the applied dynamic stress was large, the first and second stages would disappear, and the sample would directly enter the third stage (liquefaction stage), which was the case for the sample with a dynamic stress amplitude of 41 kPa.

The fourth stage was that after liquefaction, the axial stress tends to zero, the pore water pressure remained basically unchanged after being equal to the effective confining pressure, the strain accumulates in the tensile direction in an equal amplitude, and the shear strength was basically lost. This stage was called the postliquefaction stage.

5.2. Axial Dynamic Stress Test Results. The time history curve of axial dynamic stress under different dynamic stress loads is shown in Figure 2. For the convenience of comparison, the dynamic stress time history curve within 10 s is given in the figure. It can be seen from the figure that under the action of the three kinds of dynamic stresses, except for the small deviation of the zero position, the dynamic stress waveform and phase were good, and the small deviation of the zero position did not affect the final results obtained from the subsequent test data analysis. Therefore, the influence of the error caused by the axial dynamic stress on the test results could be ignored.

5.3. Axial Dynamic Strain Test Results. The time history curve of axial strain under different dynamic stress loads is shown in Figure 4. It can be seen from the figure that under the action of three dynamic stresses of 26 kPa, 33 kPa, and 41 kPa, the dynamic strain started from scratch at first, and then, the axial strain began to accumulate in the compression direction and gradually increases. After liquefaction, the strain accumulated in the tension direction in equal amplitude. During the whole vibration process, the axial strain of Fujian standard sand could develop greatly in the tension and compression direction.

5.4. Pore Water Pressure Test Results. Under the action of cyclic dynamic load, the soil sample would deform and stimulate the pore water pressure in the sample. The rise of pore water pressure would reduce the shear strength of the sample and promote the further development of shear deformation. The dynamic response of the sample was the result of the joint action of external load and pore water pressure on the soil. In engineering application and subject research, the growth model of pore water pressure was a necessary parameter model for the seismic design of liquefaction site.

Under the action of three dynamic stress amplitudes of 26 kPa, 33 kPa, and 41 kPa, the time history curve of effective pore water pressure of the sample is shown in Figure 5. It can be seen from the figure that the greater the dynamic stress was, the easier the sample was to liquefy. With the increase in vibration times, the three groups of samples met the qualitative analysis of the first three stages of liquefaction of pore

Table 2: Basic physical parameters of standard sand.

Soil sample	Minimum dry density (g.cm-3)	Maximum dry density (g.cm-3)	Nonuniformity coefficient C_u	Curvature coefficient C_c
Fujian standard sand	1.429	1.724	1.43	0.93

Table 3: The test scheme.

Consolidation ratio	Compactness	Relative density	Dynamic stress amplitude	Input waveform
$K_c = 1$	Medium density	55%	26 kPa 33 kPa 41 kPa	Sine wave

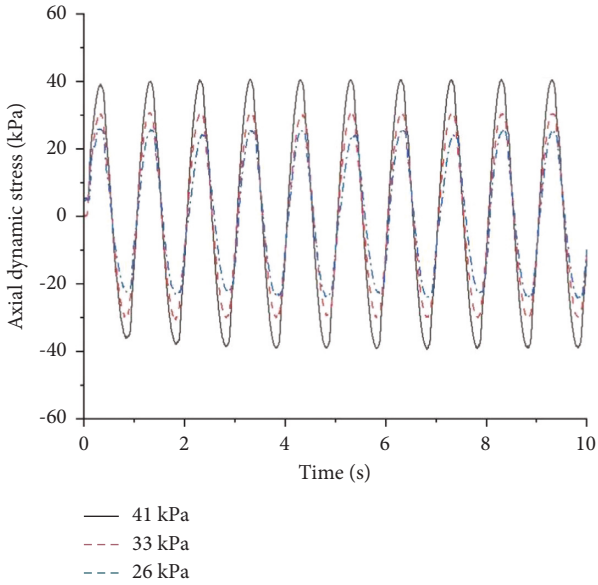

Figure 2: Time history comparison curve of axial dynamic stress of standard sand.

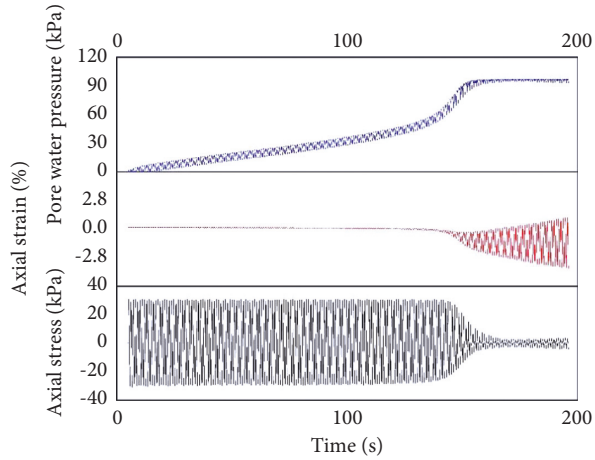

Figure 3: Time history curve of stress, strain, and pore pressure.

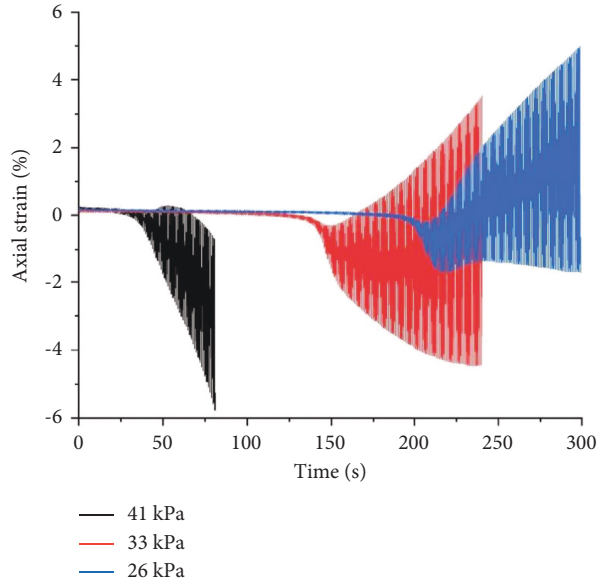

Figure 4: Comparison curve of the axial dynamic strain time history of standard sand.

water pressure growth mode in Section 5.1. That is, the pore water pressure increased rapidly at the beginning of vibration, and the growth was stable in the middle stage. When the effective pore water pressure increased to 60 kPa, it began to increase sharply and finally reached the effective confining pressure, and the sample is liquefied.

5.5. Effective Stress Path. The average effective stress deviator stress (p'-q) curve under different dynamic stress loads is shown in Figure 6. In order to facilitate comparative analysis, the three groups of results were put into one figure, as shown in Figure 7. It can be seen from Figures 6 and 7 that the effective stress paths of the three groups of tests are constrained within the same range. After liquefaction, the critical state line provided natural constraints. Under the action of different dynamic stress amplitudes, the stress path tends to zero effective stress state at a relatively different rate, indicating that the dynamic stress had a great impact on the dynamic liquefaction process of Fujian standard sand.

5.6. Stress-Strain Relationship. The stress-strain relationship curve of the sample under different dynamic stress cyclic loads is shown in Figure 8. For the convenience of observation, put the stress-strain relationship data of the sample under the action of three dynamic stresses of 26 kPa, 33 kPa, and 41 kPa into a figure, as shown in Figure 9. It can be seen from the figure that under the action of different dynamic stress

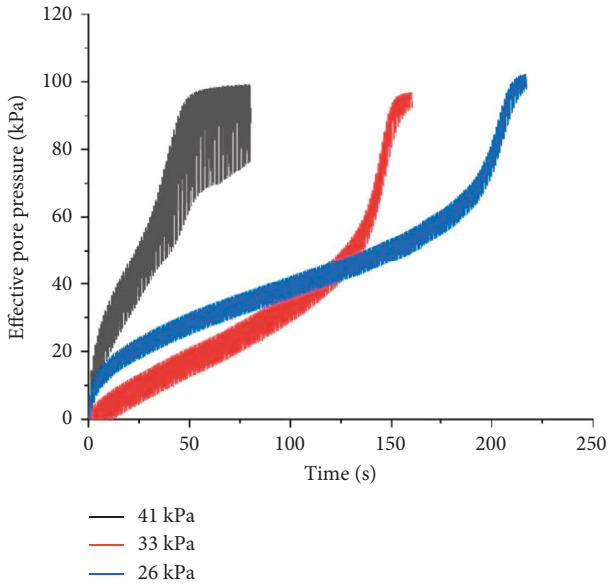

Figure 5: Time history curve of effective pore water pressure of standard sand.

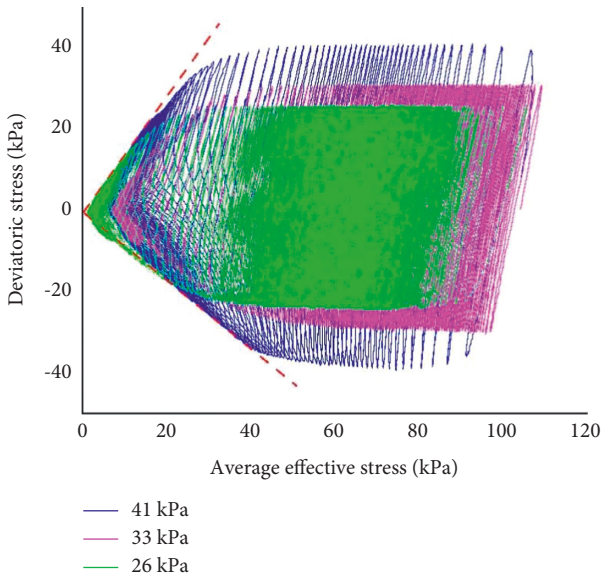

Figure 7: Effective stress path curve of standard sand (combined).

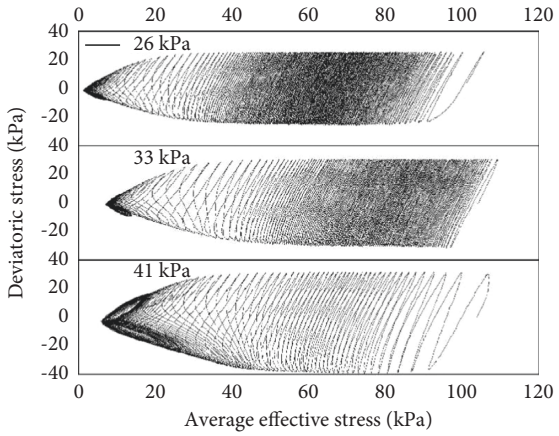

Figure 6: Effective stress path curve of the standard sand axis.

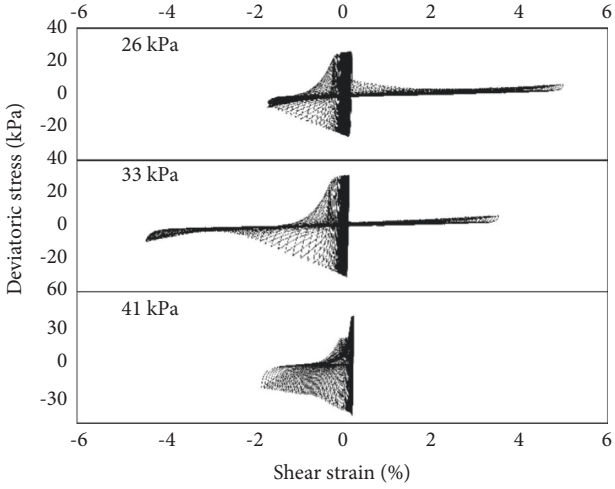

Figure 8: Stress-strain curve of standard sand (dispersion).

amplitudes, the stress-strain relationship curves of Fujian standard sand were quite different, but there were certain rules.

It can be seen from Figure 8 that under the action of three dynamic stresses, the shear stress was relatively stable before liquefaction. The amplitude and the shear strain were small. In the liquefaction stage, the stress decreased sharply until it approaches zero, and the strain increased rapidly until the specimen lost its shear strength. After liquefaction, the stress change was small and close to zero, the strain continued to increase in the tension and compression direction, the cumulative strain developed greatly, and the maximum shear strain reached 6%.

When the dynamic stress amplitude is large, the stress-strain curve of Fujian standard sand is easier to deviate to the tensile side before liquefaction, but the deformation of the compression side will develop greatly after liquefaction. When the dynamic stress amplitude is small, the stress-strain curve of Fujian standard sand is easier to lean to the compression side before liquefaction. But the deformation of the tensile side will develop greatly after liquefaction.

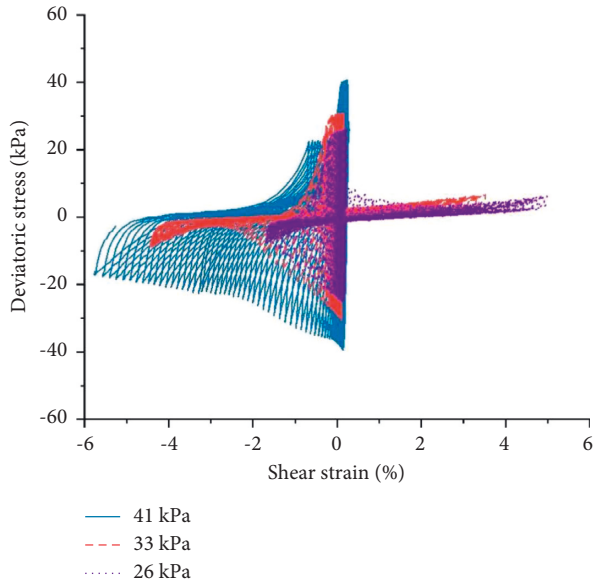

Figure 9: Stress-strain curve of standard sand (combined).

It can be seen that in the dynamic triaxial test of standard sand, the difference in dynamic stress amplitude will lead to great changes in the stress-strain relationship curve, but it has little effect on the analysis of the liquefaction dynamic characteristics of sand.

6. Conclusion

In this paper, the dynamic liquefaction test of standard sand was carried out based on KTL two-way dynamic triaxial system. The test results of dynamic stress and dynamic strain of standard sand were analyzed. The dynamic characteristics of the sample such as the pore water pressure model, effective stress path, and stress-strain relationship curve were studied. The main conclusions are as follows.

(1) With the increasing vibration times, the pore pressure increases gradually and stops rising when reaching the confining pressure, and the strain increases gradually. The whole vibration process can be basically divided into four stages.

(2) The greater the dynamic stress is, the easier the sample is to liquefy. With the increasing vibration times, the samples under different dynamic stress amplitudes meet the qualitative analysis of the first three stages of liquefaction. That is, the pore water pressure increases rapidly at the beginning of vibration, and the growth is stable in the middle stage. When the effective pore water pressure increases to 60 kPa, it begins to increase sharply and finally reaches the effective confining pressure, and then, the sample liquefies.

(3) Under the action of different dynamic stress amplitudes, the effective stress paths of the samples are constrained in the same range. After liquefaction, the critical state line provides natural constraints, but the stress path tends to zero, and the rate of effective stress state varies greatly, indicating that the dynamic stress has a great impact on the dynamic liquefaction process of Fujian standard sand.

(4) In the dynamic triaxial test of standard sand, the difference in dynamic stress amplitude will lead to great changes in the stress-strain relationship curve, but it has little effect on the analysis of the liquefaction dynamic characteristics of sand.

Data Availability

The basic data supporting the research results have been provided in this paper.

Conflicts of Interest

The authors declare that they have no conflicts of interest.

Acknowledgments

The authors gratefully acknowledge the financial support provided by the Youth Innovation Science and Technology Planning Team of Shandong Province (Grant no. 2021KJ024), the scientific research fund project of Binzhou University (Grant no. BZXYLG2119), and the Binzhou Social Science Planning Project (Grant no. 2021-SKGH-57).

References

[1] L. Tang, X. Zhang, X. Ling, H. Li, and N. Ju, "Experimental and numerical investigation on the dynamic response of pile group in liquefying ground," *Earthquake Engineering and Engineering Vibration*, vol. 15, no. 1, pp. 103–114, 2016.

[2] L. Guo, X. Liu, Z. Yang, C. Jia, W. Shi, and X. Ling, "CPT-based analysis of structured soil characteristics and liquefaction failure of the Yellow River Subaquatic Delta," *Marine Georesources & Geotechnology*, vol. 40, pp. 308–320, 2021.

[3] A. Sadrekarimi and G. A. Riveros, "Static liquefaction analysis of the fundão dam failure," *Geotechnical & Geological Engineering*, vol. 38, no. 6, pp. 6431–6446, 2020.

[4] Z. Zhou, G. Chen, and Q. Wu, "Effect of initial static shear stress on liquefaction and large deformation behaviors of saturated silt," *Rock and Soil Mechanics*, vol. 38, no. 5, pp. 1314–1320, 2017.

[5] L. Wang, "Research progress and practice of geotechnical seismic engineering and soil dynamics in China," *City and Disaster Reduction*, vol. 24, no. 4, pp. 13–26, 2021.

[6] J. Zhang, "New advances in basic theories of sand dynamics," *Chinese Journal of Geotechnical Engineering*, vol. 34, no. 1, pp. 1–50, 2012.

[7] G. Chen, *Geotechnical Earthquake Engineering*, Science Press, Beijing, China, 2007.

[8] R. O. Davis and G. Mullenger, "A rate type constitutive model for soil with a critical state," *International Journal for Numerical and Analytical Methods in Geomechanics*, vol. 2, no. 3, pp. 255–282, 1978.

[9] K. Sun and A. Zhou, "A multisurface elastoplastic model for frozen soil," *Acta Geotechnica*, vol. 16, no. 11, pp. 3401–3424, 2021.

[10] Y. Wang, J. Li, H. Deng, and R. Wang, "Investigation on unloading triaxial rheological mechanical properties of soft

rock and its constitutive model," *Yantu Lixue/Rock and Soil Mechanics*, vol. 33, no. 11, pp. 3338–3344, 2012.

[11] D. Bigoni and A. Piccolroaz, "Yield criteria for quasibrittle and frictional materials," *International Journal of Solids and Structures*, vol. 41, no. 11-12, pp. 2855–2878, 2004.

[12] K. H. Roscoe, A. N. Schofield, and A. Schofield, "Yielding of clays in states wetter than critical," *Géotechnique*, vol. 13, no. 3, pp. 211–240, 1963.

[13] Y. Li, L. Jing, Z. Shan, and F. Zhang, "Nonlinear ground response based on the theory of wave propagation in two-phase media," *Chinese Journal of Geotechnical Engineering*, vol. 37, no. 11, p. 6, 2015.

[14] F. Zhang, B. Ye, T. Noda, and K. Nakai, "Explanation of cyclic mobility of soils: approach by stress-induced anisotropy:approach by stress-induced anisotropy," *Soils and Foundations*, vol. 47, no. 4, pp. 635–648, 2007.

[15] F. Zhang, B. Ye, and G. Ye, "Unified description of sand behavior," *Frontiers of Architecture and Civil Engineering in China*, vol. 5, no. 2, pp. 121–150, 2011.

[16] B. Ye, G. Ye, and F. Zhang, "Numerical modeling of changes in anisotropy during liquefaction using a generalized constitutive model," *Computers and Geotechnics*, vol. 42, pp. 62–72, 2012.

[17] H. Fu, X. Yuan, and M. Wang, "An incremental model of pore pressure for saturated sand based on in-situ liquefaction test," *Rock and Soil Mechanics*, vol. 39, no. 5, pp. 1611–1618, 2018.

[18] Q. Dong, Z. Zhou, J. Su, X. Li, and B. Hao, "Aconstitutive model considering post-liquefaction deformation based on the logarithmic skeleton curve," *Rock and Soil Mechanics*, vol. 42, no. 7, pp. 1903–1910, 2021.

[19] R. Sun and X. Yuan, "Simplified incremental formula for estimating pore water pressure of saturated sands under anisotropic consolidation," *Chinese Journal of Geotechnical Engineering*, vol. 27, no. 9, pp. 1021–1025, 2005.

[20] K. Zhao, H. Xiong, G. Chen, H. Zhuang, and X. Du, "Cyclic characterization of wave-induced oscillatory and residual response of liquefiable seabed," *Engineering Geology*, vol. 227, pp. 32–42, 2017.

[21] Z. Zhang, T. Wang, S. Wu, and H. Peng, "Study on shear mechanical properties of mudstone with weak intercalation," *Journal of Rock Mechanics and Engineering*, vol. 41, no. 4, pp. 713–724, 2021.